Journal of Engineering Science and Technology Review 17 (3) (2024) 60-70

Research Article

JOURNAL OF
Engineering Science and Technology Review

www.jestr.org

Flexure Behavior of Corroded Reinforced Concrete Beam

Changjun Liu [1], Yage Li [1,*], Yi Shui [1], Longwen Yuan [1], Xinyan Li [1] and Kaiji Zhao [2]

[1] *CCCC Second Harbor Engineering Construction Technology Company Co., Ltd. Hubei, Wuhan 430021,China*
[2] *College of Engineering, Texas A&M University, Texas 77843, United States*

Received 11 March 2024; Accepted 5 June 2024

Abstract

The steel reinforcement within concrete beams is vulnerable to corrosion.In order to explore the flexural load-carrying capacity of beams under varying corrosion rates, a theoretical calculation and prediction model was proposed in this study. The study involved accelerated corrosion testing of three beams, with an additional beam serving as a control. A four-point bending test was conducted on all beams in accordance with predetermined corrosion rates. Strain gauges were positioned at the midspan to monitor strain data, and dial gauges were employed to measure deflection deformation at vulnerable sections. Experimental investigation was employed to ascertain the parameters that influence the deformation of a beam due to corrosion rate variations during loading, and the predictive model for the bending bearing capacity in relation to corrosion level was established. Results demonstrate the correlation between the elevated corrosion rate and the gradual increase in the average and maximal crack widths on the beam surfaces. The increase rate of maximal crack width exceeds the average, although both display a similar linear growth trend. The impact of corrosion on the initiation of crack and propagation in the test beams increase with high corrosion levels. Conversely, the effect of corrosion is limited when the corrosion rate remained below 15%. Nevertheless, once the corrosion rate exceeds 25%, a more pronounced effect becomes evident. Furthermore, the corrosion of steel reinforcement has a considerable effect on the yield and ultimate load-carrying capacity of the test beams. Upon reaching a corrosion rate of 25%, the flexural capacity of the corroded beams is found to be 54% of the uncorroded beams. This result indicates that as corrosion increases, the flexural capacity decreases linearly. This study offers a reference for accelerating the corrosion testing of reinforced concrete beams and predicting the bending bearing capacity of the corresponding corrosion level.

Keywords: Accelerated corrosion test, Corroded concrete beam, Bending test, Ultimate bearing capacity, Prediction model

1. Introduction

Reinforced concrete (RC) beams are the primary load-bearing elements in building structures, playing a critical role in modern civil engineering construction. However, concerns have long been raised regarding the durability and safety of these beams. The corrosion of RC beams is primarily influenced by environmental changes, natural disasters, and the passage of time [1-3]. Among the aforementioned factors, steel reinforcement corrosion is a major contributor to the reduction in service life. Corrosion of steel reinforcement represents a concealed and progressive phenomenon that considerably affects the mechanical performance and structural integrity of beams. The formation of an oxide layer on the surface of the steel reinforcement over time results in a reduction in the cross-sectional area and the delamination of the concrete protective layer.. This process serves to further accelerate the corrosion of the reinforcement and to weaken its bond with the concrete. As a consequence, the ultimate load-carrying capacity(ULC) is reduced. The failure to implement appropriate repair and reinforcement measures in a timely manner may result in considerable structural issues, which could compromise the safety of the buildings and potentially lead to severe safety incidents.

To address the durability requirements of RC structures, the study area of mitigating the reduction in structural mechanical performance due to steel reinforcement corrosion has emerged as a prominent field of study. This study is crucially applied in engineering projects involving RC, such as residential buildings and bridge construction. Substantial progress has been achieved in related technical study regarding the influence of steel reinforcement corrosion on the ULC of concrete beams [4-7]. Nevertheless, the multifaceted effect of steel reinforcement corrosion-induced weakening represents a considerable challenge to the accurate calculation of beam mechanical performance.

In light of this, scholars have undertaken comprehensive studies with the objective of accurately calculating the flexural performance of corroded RC beams. However, no universally accepted and unified method for determining the ULC has been found. The assessment of the extent of reinforcement corrosion within RC beams based solely on known external conditions is challenging. Furthermore, assessing the impact of cracking resulting from reinforcement corrosion on the ULC presents a multitude of challenges.

Moreover, with the advent of increasingly intricate RC constructions and denser reinforcement, reducing the computational complexity, enhancing the calculation precision, and achieving efficient ULC calculations have become of paramount importance. The accurate assessment of the flexural mechanical performance of corroded RC structures is of great engineering significance for the evaluation of durability and reliability.

To assess accurately the residual ULC of the corrosion RC components and develop targeted maintenance strategies, this study combines a substantial amount of previous experimental data. The study compares three beams in different corrosion states with one beam in a noncorroded

*E-mail address: mxyg_1122@163.com
ISSN: 1791-2377
doi:10.25103/jestr.173.08

state. Subsequently, the bending performance of the beams is tested. On the basis of the observed experimental phenomena and past test results, an empirical prediction equation for the ULC of the corroded RC beams is obtained.

2. State of the art

A substantial body of study has been conducted by scholars on the impact of corrosion on the flexural capacity of RC beams. Nevertheless, the current study on corroded RC beams is predominantly based on theoretical analysis and experiments, with the objective of investigating the ultimate bearing capacity of corroded RC beams from various perspectives. In light of the aforementioned considerations, corresponding calculation methods or models must be developed. For example, rodriguez et al. [8] ' s bending test results indicated that beams with a lower corrosion rate are more susceptible to bending failure, while beams with a higher corrosion rate and wider spacing of stirrups are more prone to shear failure. However, comprehensive studies and analyses on the evolution of crack width and prediction are lacking. Torres-Acosta et al. [9] conducted a related study on the general corrosion of steel reinforcements in a humid environment, which leads to a reduction in the cross-sectional area of the steel reinforcements. The results showed a considerable decrease in the ultimate load capacity of the test beams, highlighting the critical role of the maximal depth of steel reinforcement corrosion (PITMAX). However, it is not applicable for the case of beams with various corrosion rates and flexural capacity. Regarding the application of RC beams in practical structures, Mahdi et al. [10] reviewed experimental studies on the flexural performance of corroded prestressed concrete beams, emphasizing the potential risks of corrosion to infrastructure and industrial buildings and the degradation law of flexural strength. However, it is not suitable for predicting the degradation law of flexural strength of non-prestressed beams corresponding to different corrosion levels. Azad et al. [11] introduced an innovative two-step analysis method about predicting the residual flexural capacity of corroded RC beams. This method uses prestressed reinforcements with diameters of 16 and 18 mm to reinforce large beams, considering the size influence of the steel reinforcements to improve accuracy. The reliability of predicting the ultimate bearing capacity of corroded beams was verified through the experimental data of 48 corroded beams. However, it did not explain the prediction and calculation of the flexural capacity of beams under different corrosion rates.

Bossio et al. [12] conducted a comparative analysis by combining experimental results with complex finite element models (FEMs) to study the static behavior of corroded RC components. This study emphasized the importance of degradation caused by corrosion, especially when steel plays a dominant role in structural failure. By simulating and comparing with traditional experimental methods, the study shortened the experimental cycle and saved resources. Yuan et al. [13] established a degradation model for the stress–strain relationship of corroded steel reinforcements and the bond–slip relationship between corroded steel reinforcements and concrete through experiments. They developed an FEM for corroded beams to achieve finite element analysis. However, differences between the model predictions and actual experimental values were still observed. Xiong et al. [14] conducted experimental study on the effect of tensile zone concrete on the bending stiffness of beams after rust expansion and cracking. They emphasized the effect of tensile zone concrete on the sectional bending stiffness but ignored the influence of the early degradation of steel reinforcement bond stress. Niu et al. [15] proposed a method for calculating the load-carrying capacity of RC beams considering only the corrosion of the tensile zone steel reinforcements based on the current code. However, In the context of practical engineering, it is uncommon for the structure to be affected solely by corrosion of tension zone steel reinforcements. Fan et al. [16] analyzed the evolution law of the section curvature ductility coefficient of corroded beams with the corrosion rate of steel reinforcements and the deterioration coefficient of concrete. They derived a calculation model for the section curvature ductility of corroded beams when the bond between concrete degrades and steel reinforcements. However, the calculation load is large, and the identification process is complex. He et al. [17] did a research about the effect of load on the deformation performance of corroded steel-reinforced concrete beams through comparative tests on corroded beams under load, corroded beams without load, and a group of reference beams. The results demonstrated that the load exerted a considerable effect on the corrosion of the steel reinforcements, expediting the corrosion process and augmenting the deflection of the beam. Kashani et al. [18] comprehensively reviewed the experimental study on corroded RC components and conducted an in-depth study on the accuracy of existing FEMs in predicting the residual load-carrying capacity of these affected components. The analysis emphasized the negative effect of corrosion on ductility, leading to a decrease in ULC. The study concluded by providing suggestions for future study in this field.

Zhao [19] simulated different corrosion states in actual engineering by controlling the corroded area and corrosion rate of steel reinforcements and compared the results with the experimental results of noncorroded beams to obtain general conclusions. However, this study only simulated the corrosion development process of the tension zone reinforcement corroded beam and the compression zone reinforcement corroded beam, which is not applicable to the entire steel reinforcement framework. To understand further the microscopic changes in steel reinforcement corrosion, Green [20] comprehensively elaborated on the excellent protective influence of concrete on steel reinforcements, the corrosion mechanism of steel reinforcements, chloride-induced corrosion mechanism, carbonation corrosion, leaching-induced corrosion of steel reinforcements, and the corrosion and interference of stray current in steel reinforcements. This work provides a basis for simulating corrosion tests in the present study. Caines et al. [21] reviewed and analyzed six categories of pitting corrosion knowledge to evaluate the current depth and breadth of understanding. Zhong et al. [22] established a reliability-based quantitative design method for the durability of concrete structures in chloride environments. However, the prediction of the structural load-carrying capacity is not yet perfect.

The aforementioned research primarily concerns itself with the investigation of the influence of steel reinforcement corrosion on structural safety and the prediction of structural performance in the presence of localized corrosion. However, the consideration of comprehensive factors and finite element simulation prediction in corrosion research can still be improved. In addition, research on the overall corrosion of steel reinforcements within beams, especially the systematic and correlated study on the prediction of structural performance after corrosion of the entire framework, is

limited. The present study employs the method of electrically accelerated corrosion to simulate the corrosion of steel reinforcements in concrete. This method allows the control of parameters for the degree of corrosion of steel reinforcements, seeing of experimental phenomena relatively intuitive. The test allows the acquisition of numerous specimens within a reasonable research period and effectively simulates natural corrosion by controlling the current density. After bending performance tests were conducted on three beams at different corrosion rates and one beam blank, the ULC and crack development at different corrosion rates are recorded. On the basis of the observed experimental phenomena, a prediction equation for the ULC of corroded RC beams is derived, providing a basis for further experimental research into the complex interaction mechanism between steel reinforcements and concrete and the prediction of beam crack widths corresponding to different levels of corrosion.

The remaining part of this study is organized as follows: Section 3 elucidates the mechanism of steel reinforcement corrosion in concrete and describes the experimental process and phenomena of accelerated corrosion of steel-reinforced concrete beams. Section 4 presents the results of the flexural performance tests of the experimental beams and derives a prediction formula for the ultimate load-carrying capacity of corroded steel bar-reinforced concrete beams. The final section provides a summary of the study and draws relevant conclusions.

3. Methodology

3.1 Accelerated corrosion mechanism

The corrosion forms of steel reinforcements can be divided into two types: uniform corrosion and pitting corrosion. The difference in corrosion forms is related to the occurrence and development mechanism of corrosion. Two types of corrosion can occur on steel reinforcements and their surrounding environment: macroscopic and microscopic. Microscopic corrosion refers to the formation of numerous indistinguishable small anodes and cathodes on the surface of the steel reinforcement, resulting in relatively uniform corrosion. By contrast, macroscopic corrosion refers to the formation of different anodes and cathodes at different locations on the steel surface, resulting in localized pitting corrosion. Studies have shown that these two forms of corrosion often coexist on the steel surface, and no strict boundary exists between uniform corrosion and pitting corrosion in terms of corrosion rate [23]. Studies have indicated that when the corrosion rate is below 5%, uniform corrosion is dominant, while pitting corrosion is dominant when the corrosion rate exceeds 5% [24].

Studies have shown differences between corrosion specimens subjected to laboratory accelerated techniques and natural conditions. When specimens obtained using artificial climate environments and constant current electrochemical accelerated corrosion methods exhibit similar crack widths of corrosion expansion on the surface of components, their performance considerably deteriorates during the electrochemical process [25]. However, when the accelerated corrosion current density is controlled within a certain range, it can simulate natural corrosion conditions well[26]. El Maaddawy et al. [27] proposed that results can well represent natural corrosion when the current density of accelerated corrosion does not exceed 200 μA/cm². When evaluating in-service RC structures with corroded steel reinforcements, degradation models based on accelerated corrosion tests tend to be conservative [28].

By controlling the mass loss of the steel reinforcements, the degree of corrosion during electrification can be managed. This process involves recording the magnitude of the current obtained and the duration of electrification and applying them to relevant formulas of Faraday's law [29,30]. According to Faraday's law, (1) the amount of reducible substance deposited on the cathode in an electrochemical reaction is directly proportional to the charge passing through the electrode, and (2) the charge transfer is directly proportional to the change in the quantity of reactants [31]. The charge passing through the electrode can be calculated by using the current intensity and electrification time in the circuit (Eq. [1]). Simultaneously, by using the principle of Faraday's law, the mass loss can be determined using Eq. (2). During steel corrosion, the number of electrons lost by iron atoms varies depending on the different corrosion products. In this experiment, when the steel begins to undergo oxidation reactions, the number of electrons lost by iron atoms is assumed to be 2.

$$Q = F \cdot m = I \cdot t \tag{1}$$

In the equation, Q represents the charge passing through the specified electrode. F is the Faraday constant, which is 96,485 C/mol in this study. m represents the stoichiometric number of electrons gained or lost. I represents the current intensity in the circuit. t represents the duration of electrification.

$$\Delta m = M \frac{It}{nF} \tag{2}$$

In the equation, Δm represents the mass loss, M represents the molar mass of iron, and n represents the number of electrons released at the anode, which is 2 in this study.

3.2 Calculation of corrosion rate

In practical engineering scenarios, all the steel reinforcements inside the beam are simultaneously subjected to corrosion. Therefore, this study considers the simultaneous corrosion of all the steel reinforcements inside the beam. An accelerated method was used during the concrete mixing stage to accelerate corrosion and reduce the testing time. Specifically, a 2% concentration of NaCl solution, representing 2% of the weight of cement, was added as a partial replacement for mixing water. After pouring, the test beams were cured for 28 days under standard conditions. Accelerated corrosion was induced by immersing the beams in containers containing 5% NaCl and applying a current intensity of 0.15 A simultaneously. After immersion for 536, 1,608, and 2,680 h, corrosion rates of 5%, 15%, and 25% were respectively achieved. The corrosion level of the beam was quantified by determining the mass corrosion rate of the steel reinforcements (calculated in accordance with Eq. [3]). The mass corrosion rate of the steel reinforcements in the specimens was measured to be 0 by extracting and rusting the steel reinforcements after completing the relevant mechanical performance tests and then weighing them.

$$R_c = \frac{m_0 - m_1}{m_0} \times 100\% \tag{3}$$

In the equation, R_c represents the corrosion rate of the steel reinforcements. m_0 is the mass of the steel reinforcements before corrosion, which is calculated by multiplying the length of the steel reinforcements by the standard linear density. m_1 is the mass of the corroded steel reinforcements after rust removal.

3.3 Calculation of noncorroded RC

In accordance with the specification GB50010-2010 [32], the ultimate bearing capacity calculation for ordinary RC beams is provided. Eq. (4) in the calculation does not consider the tensile strength of concrete, as shown in Fig. 1.

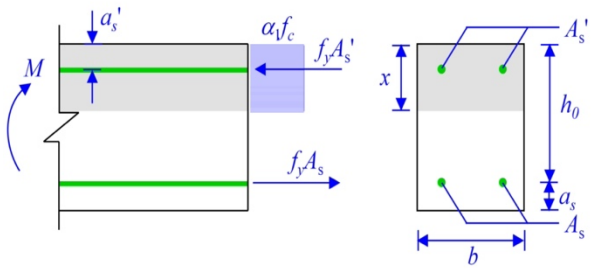

Fig. 1. Load–deflection curve of the test beam

$$M \le a_1 f_c b x \left(h_0 - \frac{x}{2}\right) + f_y' A_s' (h_0 - a_s') \tag{4}$$

The height of the compression stress zone can be calculated using Eq. (5).

$$x = \frac{f_y A_s - f_y' A_s'}{\alpha_1 f_c b} \tag{5}$$

In Eq. (5), α_1 is the reduction factor of the moment diagram, which is taken as 1.0 in this study. F_c represents the compressive strength of concrete, and f_y and f_y' represents the tensile and compressive yield strength of steel reinforcement, respectively. A_s and A_s' represent the area of tensile and compressive reinforcement, respectively. x is the height of the compression stress zone. h_0 is the effective depth, which is the distance from the centroid of the compressive reinforcement to the section edge. b is the width of the section.

3.4 Consideration of factors affecting corrosion

Studies have shown that the flexural strength of RC beams decreases with the increase in the strength of the concrete [22,33]. The decrease in flexural strength can be attributed to three main factors:

(1) Reduction in the cross-sectional area of the steel reinforcement [34]: Corrosion leads to the formation of rust, which occupies a larger volume than the original steel. This formation results in a decrease in the cross-sectional area of the steel reinforcement, thereby reducing the flexural strength.

(2) Decrease in the yield strength of the steel reinforcement [35,36]: Corrosion leads to the degradation of the material properties of the steel reinforcement, causing a decrease in the yield strength. This decrease also contributes to the reduction in flexural strength.

(3) Deterioration of the bond between corroded steel reinforcement and concrete [37,38]: Corrosion of the steel reinforcement can weaken the bond between the corroded steel and adjacent concrete. This reduction in bond strength leads to a decrease in the composite action between the steel reinforcement and concrete, further reducing the contribution of the steel reinforcement to the flexural strength of the beam.

The first two factors (reduction in steel cross-sectional area and decrease in yield strength) can be directly incorporated into the calculation formula. However, the third factor (reduction in bond strength) must be included in the predictive model through empirical parameter fitting. The discussion on these three factors is as follows:

(1) Reduction in steel cross-sectional area

The corrosion of steel reinforcement leads to the formation of an oxide layer on the surface of the steel, resulting in a reduction in the effective cross-sectional area. This reduction can be quantified by calculations related to the degree of corrosion, as shown in Eq. (6).

$$A_{sc} = (1 - R_c) A_s \tag{6}$$

In the equation, A_{sc} and A_s represent the cross-sectional areas of the steel reinforcement before and after corrosion, respectively.

(2) Corrosion leads to a decrease in the yield strength of the steel reinforcement

As corrosion progresses, the change of the properties of the rebar, which includes a reduction in yield strength, ultimate strength and elongation, leads to a reduction in their respective values. The length of the yield plateau may be shortened, and in many cases, it may completely disappear. Specifically, the reduction in yield strength of corroded steel reinforcement can be quantified using Eq. (7).

$$f_{yc} = \beta(R_c) f_y \tag{7}$$

Where f_y and f_{yc} represent the yield strength of the steel reinforcement before and after corrosion, respectively. $\beta(R_c)$ is the corrosion-induced reduction factor. Experimental results have shown that a considerable decrease in yield strength has a considerable effect on the yield and ULC of RC beams. As the yield strength decreases, the steel reinforcement is more prone to yield under loading, resulting in a decrease in the flexural strength and ULC of the beam. Therefore, accurately determining the reduction in yield strength caused by corrosion is essential for predicting the behavior of corroded RC beams and ensuring the safety and effectiveness of structures in practical applications.

Fang [39] investigated the yield strength, ultimate strength, ductility, and corrosion rate of corroded steel reinforcement and established empirical correlations between these variables. The relationship between f_y, f_{yc}, and R_c is shown in Eq. (8).

$$f_{yc} = (1 - 0.013 R_c) f_y \tag{8}$$

(3) Deterioration of bond strength between corroded steel reinforcement and concrete

This deterioration can be quantified by utilizing Eq. (9).

$$\tau = \frac{N}{\pi d l}, \tag{9}$$

Where N and d represent the tensile force and bond strength of the steel reinforcement, respectively. l denotes the bond length between the steel reinforcement and concrete.

The study results indicate that the bond strength between the steel reinforcement and concrete increases and then decreases with the increase in steel reinforcement corrosion (R_c) [40, 41]. When R_c is low, the influence of corrosion on the bond strength of specimens is minimal. In many cases, a slight increase may even occur. This increase can be attributed to the early stages of the corrosion process, where corrosion by-products fill the gaps between the steel reinforcement and concrete, increasing radial pressure and indirectly enhancing the bond strength [42, 43]. However, as the corrosion rate accelerates the expansion of corrosion products on the steel reinforcement surface and erosion of ribbing gradually lead to a decrease in bond strength. Additionally, factors such as test methods, thickness of protective layer, diameter of steel reinforcement, transverse steel confinement, loading conditions, etc., collectively affect the bond strength [44].

Therefore, the relationship between corroded steel reinforcement and concrete can be represented by Eq. (10).

$$\tau_c = \gamma(R_c)\tau \tag{10}$$

Where $\gamma(R_c)$ is the reduction factor associated with R_c.

Almusallam [45] conducted an in-depth study on the influence of different levels of corrosion on bond strength. The study introduced a reduction coefficient for ribbed steel reinforcement bond strength that is related to the degree of corrosion. The results showed that as the corrosion level of the steel reinforcement (R_c) increased, the bond strength initially increased and then decreased. In cases of lower corrosion levels, the presence of corrosion by-products filled the gaps between the steel reinforcement and concrete, increasing the radial pressure and thus enhancing the bond strength. However, as the corrosion rate continued to rise, the bond strength gradually decreased due to the expansion of corrosion by-products and the loss of ribs on the surface of the threaded steel.

A reduction factor for bond strength is introduced in the literature to express the relationship between the bond strength of ribbed reinforcement and the degree of corrosion accurately. This reduction factor is quantified by Eq. (11).

$$\gamma(R_c) = \begin{cases} 1 + 21R_c & R_c \le 0.017 \\ 1.359 - 0.11R_c & R_c > 0.017 \end{cases} \tag{11}$$

3.5 Prediction of corroded RC and ULC

As the degree of corrosion deepens, the yield strength of the reinforcement and the bond performance between the reinforcement and concrete correspondingly decrease. Under the condition of bending load on the specimen, two potential failure modes may occur: yielding of the reinforcement or bond slip, as shown in Eq. (12–14).

$$\begin{cases} N_{yc} \ge \Gamma_c & bond-slip \\ N_{yc} < \Gamma_c & yield \end{cases} \tag{12}$$

$$N_{yc} = f_{yc}\frac{\pi d^2}{4} \tag{13}$$

$$\Gamma_c = \tau_c \pi d l_b \tag{14}$$

In the equation, N_{yc} represents the yield stress of the corroded reinforcement. Γ_c is the total bond strength. f_{yc} represents the yield strength of the tensile stress reinforcement. d is the diameter of the tensile reinforcement. τ_c is the bond strength of a single reinforcement. l is the calculated bond length of the tensile reinforcement. The height of the compressive stress zone is calculated by Eq. (15).

$$x = \frac{\sum_{i=1}^{n_t} F_{t,i} - \sum_{i=1}^{n_c} F_{c,i}}{\alpha_1 f_c b} \tag{15}$$

In the equation, F_{ti} and F_{ci} respectively represent the total forces in the tensile stress area and compressive stress area of the reinforcement, taking the smaller value between f_{yc} and f_{tc} . Here, n_t and n_c respectively indicate the number of reinforcements in the tensile stress area and compressive stress area.

3.6 Test verification

In this study, four RC beams were prepared, each with a cross-sectional dimension of 200 mm × 300 mm. The degree of corrosion (0%, 5%, 15%, 25%) was used as a variable for the test beams. The test beams were respectively named BF-0/5/15/25, where 0, 5, 15, and 25 represent the designed corrosion levels of the beams. The concrete mix ratio for the beam specimens was cement: sand: crushed stone: water = 1:2.5:3.4:0.6. Simultaneous with the preparation of the test beams, three sets of material property cube specimens were cast. After a standard curing period of 28 days, the average compressive strength of the specimens was 17.2 MPa.

The detailed information of the test beams is shown in Fig. 2. The shear reinforcement in the beams consists of 6 mm HPB235 grade reinforcing steel reinforcement (with a yield strength of 325 MPa), while the longitudinal reinforcement includes 16 and 8 mm HRB335 grade reinforcing steel reinforcement (with a yield strength of 405 MPa), respectively arranged in the tension and compression zones.

The accelerated corrosion process is shown in Fig. 3. After completion of the corrosion process, displacement-controlled loading was applied to the test beams. A stepwise loading method was used, continuing until the midspan displacement increased by 2 mm. At each loading stage, the development of strain and cracks was recorded. The loading and measurement process for the test beams is shown in Fig. 4.

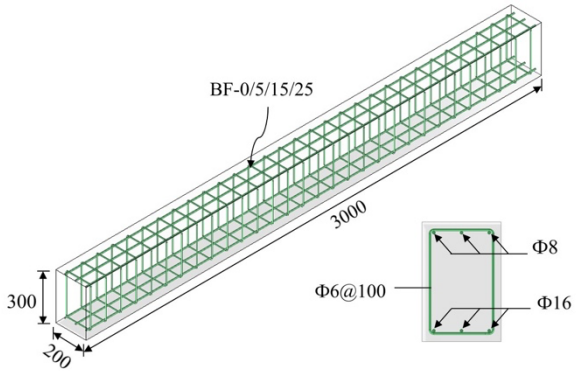

Fig. 2. Detailed dimensions and reinforcement arrangement of the test beams (units: mm)

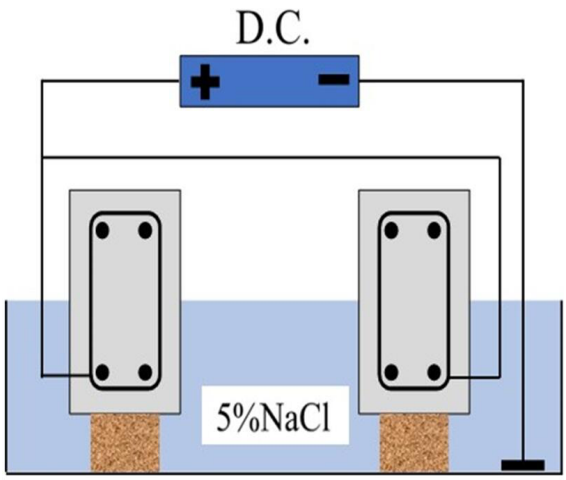

Fig. 3. Accelerated corrosion of the test beams

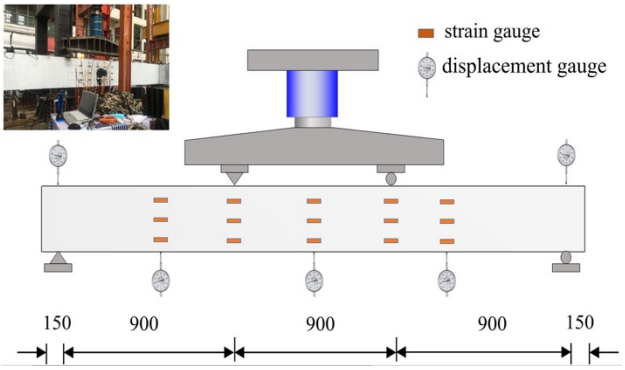

Fig. 4. Loading and measurement scheme for the test beams

4. Result analysis and discussion

4.1 Experimental settings

The development of corrosion cracks originates from the accelerated corrosion of reinforcement. The by-products apply radial tensile stresses on the surrounding concrete. When the stress exceeds the tensile strength of the concrete, it leads to radial cracks at the interface between the reinforcement and the concrete. As the corrosion progresses, the radial cracks propagate toward the concrete surface until they reach the protective cover crack. The observed corrosion cracks on the surface of the test beams exhibit a consistent morphology, characterized by fine cracks distributed around the reinforcement. The positions of the widest cracks seem to be random.

During the entire accelerated corrosion test, corrosion by-products were observed flowing out through the pores of the concrete to the surface of the specimens, primarily displaying reddish-brown or brown color. As the accumulation of corrosion by-products increased, corrosion cracks began to appear on the surface of the beams, leading to more overflow at these crack locations. Fig. 5 illustrates the distribution and width of corrosion cracks in each beam after completion of the corrosion process.

As shown in Fig. 5, the cracks observed in Beam BF-5 are relatively fine, characterized by small widths and a local distribution on the beam surface. This result can be attributed to the low corrosion level, where the formation of corrosion by-products has not yet led to remarkable expansion of the steel reinforcement (Fig. 5a). Compared with BF-5, as the corrosion by-products gradually increase, the force of expansion of the reinforcement also increases, applying increased radial pressure to the concrete. This increase results in a remarkable expansion and widening of corrosion cracks in BF-15, which become wider and longer and begin to extend more prominently and broadly on the surface of the test specimen. At this point, cracks start to form along the direction of the longitudinal reinforcement (Fig. 5b). The corrosion cracks in Beam BF-25 exhibit evident expansion and distribution, forming a dense network of medium and small cracks that fill the beam surface. At this stage, the width of the cracks remarkably increases, and they are no longer confined to the surface but extend partly into the thickness direction of the beam (Fig. 5c).

Table 1 shows the actual corrosion rates of each beam, the maximum crack width (w_{max}), and the average crack width (w_{avr}). w_{max} and w_{avr} were measured after corrosion was completed. As shown in Table 1 and Fig. 6, with the increase in corrosion rate, w_{max} and w_{avr} gradually increased. The increase rate of w_{max} is greater than that of w_{avr} , but overall, they show approximately linear growth trends.

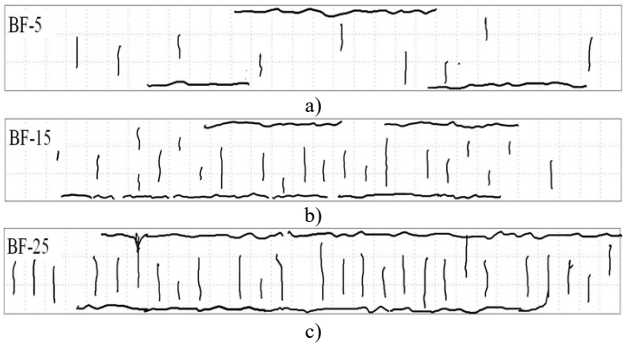

Fig. 5. Distribution of corrosion cracks

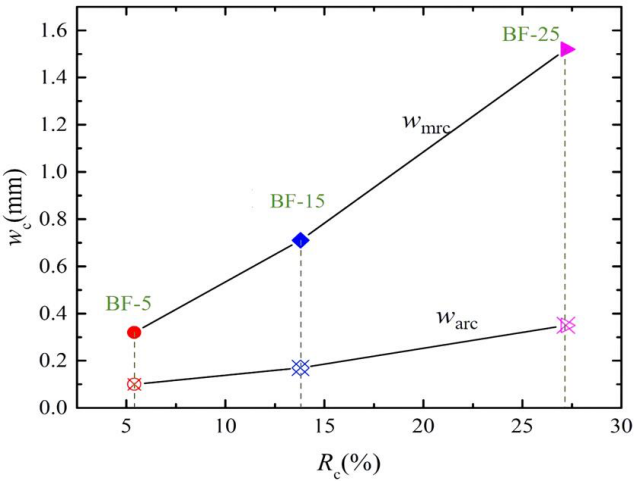

Fig. 6. Trend of corrosion-induced cracks

Table 1. Details of cracks caused by corrosion

Item	Actual R_c /%	w_{avr} /mm	w_{max} /mm
BF-5	5.4	0.10	0.32
BF-15	13.8	0.17	0.71
BF-25	27.2	0.35	1.52

Note: R_c represents the corrosion rate.

As shown in Table 2, this study conducted tests on a reference beam and three corroded beams, and the test results were calculated using Eqs. (12–15). The overall calculation results basically meet the prediction requirements and have a

certain safety margin. However, when the corrosion level of the test beams is high, major errors were observed. On the one hand, this difference can be attributed to the substantial weakening of the bond strength at high corrosion levels, making it difficult to predict the synergistic coefficient between them accurately. On the other hand, in the case of extensive corrosion, the failure mode transitions to a shear-bending composite failure, and simple bending calculations are insufficient to predict the failure behavior accurately, leading to increased calculation errors.

Table 2. Calculation result

No.	Actual R_c /%	F_u	F_{pu}	F_{pu} / F_u
BF-0	0	178	160.4	0.90
BF-5	5.4	160.9	158.9	0.99
BF-15	13.8	134.1	122.7	0.91
BF-25	27.2	95.3	82.7	0.87

4.2 Load–displacement response

Fig. 7 shows the load–displacement curve, with the respective ultimate loads and crack initiation loads detailed in Table 3. The response displacement of the test beams to the load is shown in Fig. 7, manifesting in three distinct stages:

(1) Elastic stage (before point A): In the initial loading stage before point A, the load–displacement curve remains linear, and no evident load crack extension is observed on the surface of the beam.

(2) Crack propagation stage (AB): As the load increases, the slope of the curve changes at point A, with a slight decrease in slope. In this stage, cracks rapidly widen and propagate, and as point B approaches, smaller cracks penetrate the height of the test beam.

(3) Yielding stage (after B): When the test beam is loaded to point B, a considerable deviation occurs in the slope of the curve, indicating that the reinforcing steel inside the beam has reached its yield strength. At this point, the deflection of the curve continues to rise, but it becomes impractical to apply further loads, indicating the end of the test.

Fig. 7a, Fig. 7b, Fig. 7c and Fig. 7d respectively record the load-displacement curves of the four test beams. By comparing the load–displacement curves of the four test beams (Fig. 7e) and summarizing the key load values in Table 3 and Fig. 7f, notable conclusions can be drawn. In the initial loading stage, the curves of the four beams maintain similar slopes, with deviations occurring at point A. Among BF-0, BF-5, and BF-15, the deflections at point A are similar, with BF-5~25 being 0.99, 0.96, and 0.73 times that of BF-0, respectively. The linear elastic limit of BF-25 is 37.8 kN, which deviates considerably from the other specimens. This deviation indicates that when the corrosion rate (R_c) is within 15%, the effect of corrosion cracking on RC beams is relatively small. However, as the corrosion rate increases (R_c > 25%), the corrosion effect becomes more pronounced.

By contrast, considerable differences in the yield loads (F_y) and ultimate loads (F_u) are observed among the four beams. The F_y of the corroded beams is 0.89, 0.75, and 0.51 times that of the uncorroded beam, and F_u is 0.9, 0.75, and 0.54 times, respectively. This result highlights the substantial effect of corrosion on F_y and F_u, as shown in Fig. 7f, where the linear decrease trend is apparent.

Although randomness occurs during corrosion (such as the variability in the degree of steel corrosion and its distribution and the discrete effect on bearing capacity), the trend of decreasing bearing capacity with increasing corrosion rate remains apparent. Under the same reinforcement diameter, the bearing capacity of the uncorroded control specimens is remarkably higher than that of the accelerated corrosion control specimens. As R_c increases, the F_y and F_u of the corroded specimens decrease considerably, and the load–deflection curve shows a more systematic trend of decreasing from high to low.

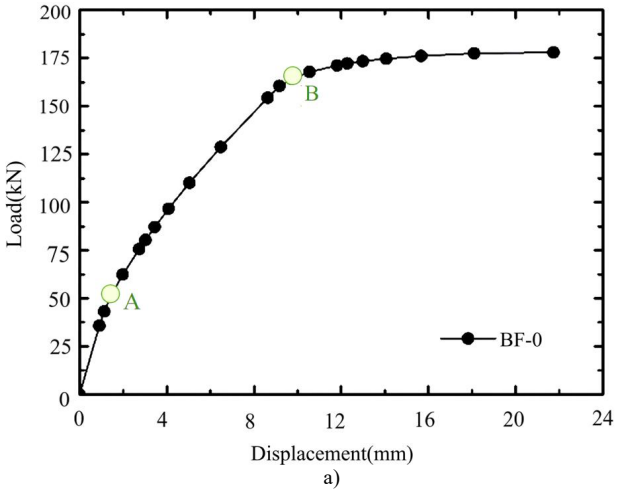

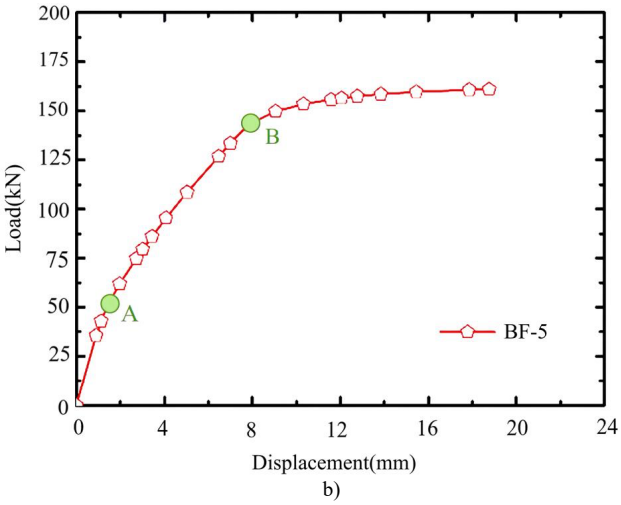

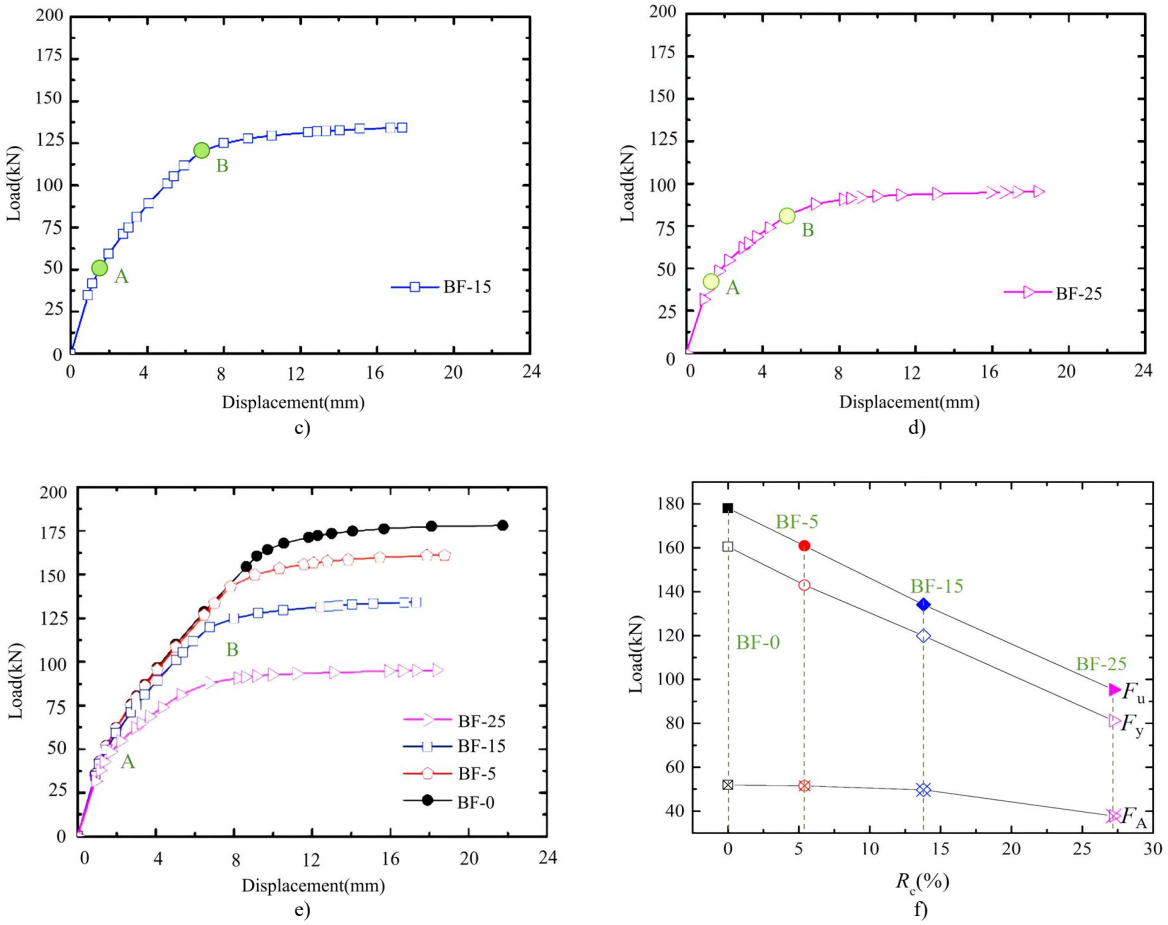

Fig. 7. Load–deflection curves of the test beams

Table 3. Summary of key load values

No.	Actual R_c /%	F_u /kN	F_{ui} /F_{u0}	F_y /kN	F_{yi} /F_{y0}	F_A /kN	F_{Ai} / F_{A0}
BF-0	0	178	1.00	160.5	1.00	51.9	1.00
BF-5	5.4	160.9	0.90	143	0.89	51.5	0.99
BF-15	13.8	134.1	0.75	119.9	0.75	49.7	0.96
BF-25	27.2	95.3	0.54	81.2	0.51	37.8	0.73

4.3 Failure modes and crack distributions

The crack distribution after beam failure is shown in Fig. 8. In Fig. 8a, when R_c = 0% in BF-0, the tensile zone cracks are uniformly distributed, with more vertical cracks, representing a typical flexural failure mode. The Fig. 8b shows that as R_c increases, the vertical cracks decrease, but the crack spacing increases because after crack initiation, the cracks gradually merge and penetrate with the initial corrosion cracks, resulting in limited evidence of crack development in other areas after stress release. BF-15 and BF-25 exhibit more evident diagonal cracks (Fig. 8c and 8d), extending from the support end to the loading point. This observation indicates a transition of the failure mode from bending to shear.

The crack distribution shown in Fig. 8 reveals that the positions of vertical cracks coincide with the locations of stirrups, indicating that the corrosion expansion of the stirrups during electrolytic corrosion has caused damage to the concrete. The failure of the test beams often occurs at locations with severe initial vertical cracks, suggesting that the vertical cracks caused by stirrup corrosion have a more considerable effect on structural performance than the diagonal cracks caused by longitudinal reinforcement. The corrosion expansion of the stirrups leads to local damage of the concrete beam section and even the formation of vertical cracks, weakening the ultimate bearing capacity of the beam. This results in a relatively weaker beam section, leading to the formation and continued development of vertical cracks under load, until failure. During the failure process, the longitudinal diagonal cracks formed by corrosion intersect with the longitudinal induced cracks caused by load action, causing the vertical cracks at the bottom of the beam to expand rapidly, and extensive spalling of the concrete in the tension zone.

In summary, the corrosion of stirrups leads to a decrease in the mechanical properties of steel and concrete, ultimately resulting in a reduction in the ULC of RC structures. During loading, the vertical cracks produced by the expansion due to stirrup corrosion gradually develop into the main cracks, ultimately leading to failure. The extent and uniformity of stirrup corrosion directly affect the ultimate bearing capacity, failure mode, and deformation performance of RC beams.

The test results indicate that all test beams failed due to bending. When the corrosion rate was 0%, the vertical cracks in the tension zone were relatively evenly distributed with an increased number of cracks. As R_c increased, the number of vertical cracks gradually decreased, but the crack spacing increased. With the increase in R_c, the test beams transitioned

from a properly reinforced and flexural failure mode to a failure mode similar to that of under-reinforced beams.

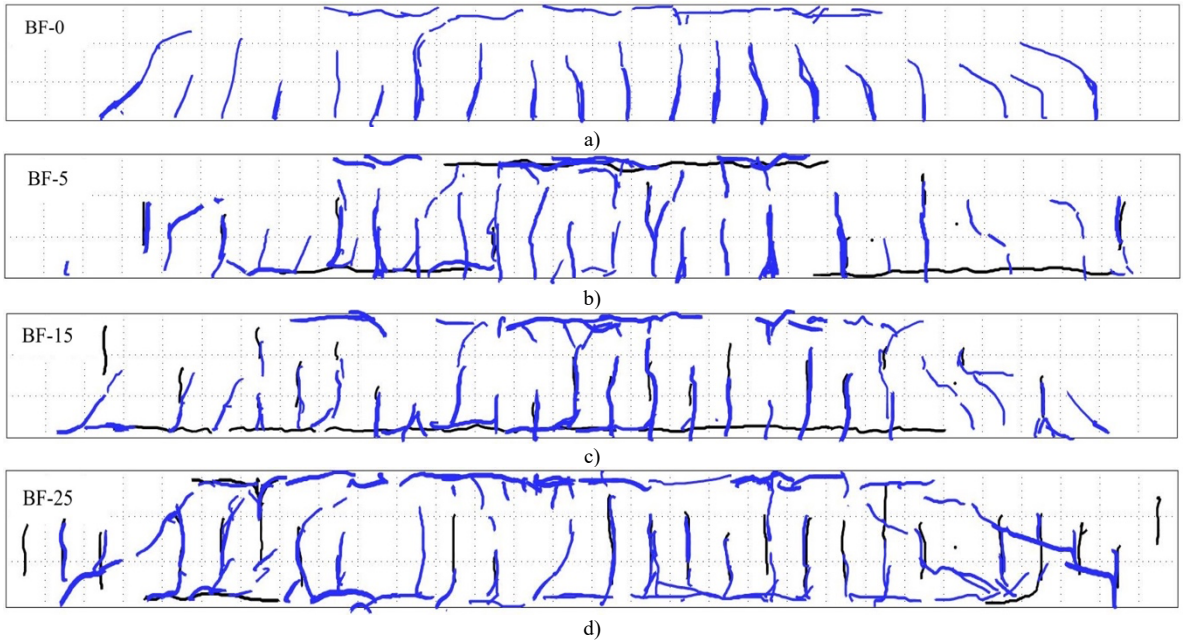

Fig. 8. Crack distribution diagram of the test beams

For test beams with relatively low R_c values, their failure process and behavior are relatively similar to those of uncorroded flexural members. This similarity indicates that when steel reinforcement undergoes corrosion but has not yet reached the degree of corrosion-induced expansion and cracking, the load-bearing performance of flexural members remains relatively stable during the cracking stage.

By contrast, for test beams with high corrosion rates, longitudinal close-coupled stresses (CCS) appear along the direction of the longitudinal steel reinforcement. In comparison with specimens without CCS, considerable differences are observed in their load-bearing characteristics. The presence of CCS considerably weakens the overall integrity of the RC structure, and the presence of chloride ions reduces the tensile strength of the concrete. Therefore, the cracking load of the test beams is considerably reduced, with cracks appearing at a certain height and extending to the positions of corrosion-induced crack expansion. After further loading, cracks develop into vertical cracks but do not exceed the corrosion-induced expansion cracks. Instead, they propagate toward the compressive stress region away from the original crack position.

As R_c increases, the location of diagonal cracks is closer to the midspan of the beam compared with specimens without R_c . Corroded beams suffer severe losses in terms of reinforcement cross-section, strength, and concrete bond strength. Under the same load, the crack width of corroded beams is larger than that of uncorroded beams, and the failure load is considerably lower than that of uncorroded beams.

5. Conclusions

To investigate the effect of different corrosion rates on the crack width of beam bodies and to reveal the ultimate bearing capacity of corroded RC beams under different corrosion rates, this study conducted corrosion tests on three RC beams and performed a comparative test on an additional beam. The results of the aforementioned experiments were then subjected to flexural performance tests on the test beams. A predictive formula for the ultimate bearing capacity of corroded RC beams was derived. The following conclusions could be drawn:

(1) With the increase in corrosion rate, the average crack width and the maximum crack width on the surface of the test beams gradually increase. The increase rate of the maximum crack width is greater than that of the average crack width, but overall, they show an approximately linear growth trend.

(2) When the corrosion degree of the test beams is within 15%, the effect on the cracking and crack propagation of the RC beams is limited. However, when the corrosion level is higher (>25%), the observed effects are more pronounced. By contrast, corrosion has a considerable effect on the yielding and ultimate load capacity of the test beams, and it shows a linear decrease trend with the increase in corrosion.

(3) The increase in corrosion degree leads to a corresponding decrease in the yield strength of the reinforcement and the bond performance between the reinforcement and the concrete.

This study combines indoor experiments with theoretical research in order to derive a prediction formula for the ultimate load-carrying capacity of corroded steel reinforcement RC beams. In summary, the calculated results generally meet the prediction requirements and exhibit a certain level of safety margin. The calculation of the ultimate load-carrying capacity of corroded steel bar reinforced concrete beams provides a valuable reference point for future studies. Nevertheless, significant discrepancies arise when the degree of corrosion in the test beams is considerable. On the one hand，this is due to the significant reduction in bond strength at higher levels of corrosion, which makes it difficult to accurately predict the synergistic coefficient between them. On the other hand, in the event of extensive corrosion, the failure mode shifts to a combined shear-bending failure, rendering the application of simple bending calculations inadequate for the accurate prediction of failure behavior. Consequently, future research should aim to control the level of corrosion and the corrosion area in accelerated corrosion

tests, in order to achieve more accurate calculations of the ultimate load-carrying capacity of corroded steel bar reinforced concrete beams.

Acknowledgements

This study was funded by the Second Harbor Engineering Company of China Communications Construction Company, with project number [JSKF-20200810-027].

References

[1] M. Akiyama, D. M. Frangopol, and H. Ishibashi, "Toward life-cycle reliability-, risk-and resilience-based design and assessment of bridges and bridge networks under independent and interacting hazards: emphasis on earthquake, tsunami and corrosion," *Struct. Infrastruct.,* vol. 16, no. 1, pp. 26-50, May. 2019.

[2] L. Zhang, L. Sun, and L. Dong, "Experimental study on the relationship between the natural frequency and the corrosion in reinforced concrete beams," *Adv. Mater. Sci. Eng.*, vol. 2021, pp. 1-10,Jul. 2021.

[3] E. Verstrynge, V. S. Charlotte, V. Eline, and W. Martine, "Steel corrosion damage monitoring in reinforced concrete structures with the acoustic emission technique: A review," *Constr. Build. Mater.*, vol. 349, Sep. 2022, Art. no. 128732.

[4] Y. C. Ou, L. L. Tsai, and H. H. Chen, "Cyclic performance of large-scale corroded reinforced concrete beams," *Earthq. Eng. Struct.,* vol. 41, no. 4, pp. 593-604, Jun. 2011.

[5] M. Zhang, N. Nishiya, M. Akiyama,S. Lim, and K. Masuda, "Effect of the correlation of steel corrosion in the transverse direction between tensile rebars on the structural performance of RC beams," *Constr. Build. Mater.*, vol. 264, Dec. 2020, Art. no.120678.

[6] A. Alaskar, A. S. Alqarni, G. Alfalah, A. K. EI-Sayed, and H. Mohammadhosseini , "Performance evaluation of reinforced concrete beams with corroded web reinforcement: Experimental and theoretical study," *J. Build. Eng.*, vol. 35, Mar. 2021, Art. no.102038.

[7] S. Lim, M. Akiyama, and D. M. Frangopol, "Assessment of the structural performance of corrosion-affected RC members based on experimental study and probabilistic modeling," *Eng. Struct.*, vol. 127, no. 189-205, Nov. 2016.

[8] J. Rodriguez, L. M. Ortega, and J. Casal, "Load carrying capacity of concrete structures with corroded reinforcement," *Constr. Build. Mater.*, vol. 11, no. 4, pp. 239-248, Jun. 1997.

[9] A. A. Torres-Acosta, S. Navarro-Gutierrez, and J. Terán-Guillén, "Residual flexure capacity of corroded reinforced concrete beams," *Eng. Struct.*, vol. 29, no. 6, pp. 1145-1152, Jun. 2007.

[10] K. Mahdi, B. Armando,F. Barbara, and I. Stefania , "Residual flexural capacity of corroded prestressed reinforced concrete beams," *Metals-basel*, vol. 11, no. 3, pp. 442, Mar. 2021.

[11] A. K. Azad, S. Ahmad, and B. H. A. Al-Gohi, "Flexural strength of corroded reinforced concrete beams," *Mag. Concrete. Res.*, vol. 62, no. 6, pp. 405-414, Jun. 2010.

[12] A. Bossio, S. Imperatore, and M. Kioumarsi , "Ultimate flexural capacity of reinforced concrete elements damaged by corrosion," *Buildings-BASEL*, vol. 9, no. 7, pp. 160, Jul. 2019.

[13] Y. Yuan, F. Jia, and Y. Cai, "The structural behavior deterioration model for corroded reinforced concrete beams," *China Civil. Eng. J.*, vol. 34, no. 3, pp. 47-52, Jun. 2001.

[14] G. Xiong, Y. Liu, and H. Xie, "Contribution of concrete located in tension zone to ultimate moment capacity of RC beams," *Industrial. Constru.*, vol. 29, no. 12, pp. 3, Dec. 1999.

[15] D. Niu, M. Lu, and Q. Wang, "Research on calculation method of the bending capacity of corrosive reinforced concrete beams," *Building. Struct.*, vol. 32, no. 10, pp. 14-17, Oct. 2002.

[16] Y. Fan and J. Zhou, "Study on ductility of corroded reinforced concrete beam," *J. Hydraul. Eng.*, pp. 112-116, Sep. 2003.

[17] S. He and J. Gong, "Experimental studies on steel bar corrosion and serviceability of reinforced concrete beam under service loading," *J. Southeast Univ.*, vol. 34,no. 4, pp. 474-479, Jul. 2004.

[18] M. Kashani , J. Maddocks, and E. A. Dizaj, "Residual capacity of corroded reinforced concrete bridge components: State-of-the-art review," *J. Bridge. Eng.*, vol. 24, no. 7, pp. 03119001, Jul. 2019.

[19] X. Zhao, "Experimental study on the performance of corroded Reinforced Concrete beams," Ph.D. dissertation, College. Civil. Eng., Hunan Univ., Changsha, Hunan, China, 2006.

[20] W. K. Green, "Steel reinforcement corrosion in concrete–an overview of some fundamentals," *Corros. Eng. Sci. Techn.*, vol. 55, no. 4, pp. 289-302, Jun. 2020.

[21] S. Caines, F. Khan, and J. Shirokoff, "Analysis of pitting corrosion on steel under insulation in marine environments," *J. Loss. Prevent. Proc.*, vol. 26, no. 6, pp. 1466-1483, Nov. 2013.

[22] X. Zhong, W. Jin, and B. Zhang, "Durability Design Method of Concrete Structures under Chloride Environment," *J. Build. Mater.*, vol. 19, no. 3, pp. 544-549, Jun. 2016.

[23] F. O. Pessu, "Investigation of pitting corrosion of carbon steel in sweet and sour oilfield corrosion conditions: a parametric study," Ph.D. dissertation, School Mechanical Eng., Leeds Univ, Leeds, UK, 2015.

[24] J. Zhu, "Shear capacity analysis of reinforced beam strengthened with fiber reinforced polymer considering the feature of rebar corrosion," M.S. thesis, Institute Architect. Eng., Zhejiang Univ., Hangzhou, Zhejiang, China, 2013.

[25] Y. Yuan, X. Zhang, and Y. Ji, "A comparative study on structural behavior of deteriorated reinforced concrete beam under two different environments," *China Civil Eng. J.*, vol. 39, no. 3, pp. 5, Mar. 2006.

[26] H. Lin, "Experimental study on the bond behavior of corroded reinforced concrete under monotonic or repeated loading," Ph.D. dissertation, Institute. Architectural. Eng., Zhejiang Univ., Hangzhou, Zhejiang, China, 2017.

[27] T. A. El Maaddawy and K. A. Soudki, "Effectiveness of impressed current technique to simulate corrosion of steel reinforcement in concrete," *J. Mater. Civil. Eng.*, vol. 15, no. 1, pp. 41-47, Jan. 2003.

[28] W. Zhu and R. Francois, "Corrosion of the reinforcement and its influence on the residual structural performance of a 26-year-old corroded RC beam," *Constr. Build. Mater.*, vol. 51, pp. 461-472, Jan. 2014.

[29] X. Yang, T. Wu, and Y. Chen, "Relationship of corrosion of concrete reinforcement to accelerated corrosion current," *Proc. Inst. Civ. Eng-co.*, vol. 172, no. 5, pp. 263-268, Oct. 2019.

[30] S. F. U. Ahmed, M. Maalej, and H. Mihashi, "Cover cracking of reinforced concrete beams due to corrosion of steel," *Aci. Mater. J.*, vol. 104, no. 2, pp. 153, Apr. 2007.

[31] W. Cui, Z. Shi, G. Song, H. Lin, and C. CAO, "Electrochemical study on the reinforced concrete during curing," *Corros. Sci. Protect. Techn.*, vol. 10,no. 4, pp. 202-207, Jul. 1998.

[32] *Code for design of concrete structures*, GB50010-2010, 2010.

[33] B. Kamil, Y. Hakan, B. A. Pekrioglu, and K. Atila, "Effect of corrosion on flexural strength of reinforced concrete beams with polypropylene fibers," *Constr. Build. Mater.*, vol. 185, pp. 574-588, Oct. 2018.

[34] W. Zhang, B. Zhou, X. Gu, and H. Dai, "Probability distribution model for cross-sectional area of corroded reinforcing steel bars," *J. Mater. Civil. Eng.*, vol. 26, no. 5, pp. 822-832, Jul. 2014.

[35] H. Chen, J. Zhang, J. Yang, and F. Ye, "Experimental investigation into corrosion effect on mechanical properties of high strength steel bars under dynamic loadings," *Int. J. Corros.*, vol. 2018, pp. 1-12, Jan. 2018, Art. no. 7169681.

[36] W. Zhang, X. Song, X. Gu, and S. Li, "Tensile and fatigue behavior of corroded rebars," *Constr. Build. Mater.*, vol. 34, pp. 409-417, Sep. 2012.

[37] H. S. Lee, T. Noguchi, and F. Tomosawa, "Evaluation of the bond properties between concrete and reinforcement as a function of the degree of reinforcement corrosion," *Cement. Concrete. Res.*, vol. 32, no. 8, pp. 1313-1318, Aug. 2002.

[38] X. Wang and X. Liu, "Modeling bond strength of corroded reinforcement without stirrups," *Cement. Concrete. Res.*, vol. 34, no. 8, pp. 1331-1339, Aug. 2004.

[39] L. Fang and Y. Zhou, "Experimental study on flexural behavior of corroded reinforced concrete slabs with HRB500 bars," *J. Hunan Univ.: Natural Sci.*, vol. 47, no. 11, pp. 84-94, Nov. 2020.

[40] M. Alhawat and A. Ashour, "Bond strength between corroded steel reinforcement and recycled aggregate concrete," *Structures*, vol. 19, pp. 169-385, Jun. 2019.

[41] Y. Zhao, H. Lin, K. Wu, and W Jin, "Bond behavior of normal/recycled concrete and corroded steel bars," *Constr. Build. Mater.*, vol. 48, pp. 348-359, Nov. 2013.

[42] F. Tondolo, "Bond behavior with reinforcement corrosion," *Constr. Build. Mater.*, vol. 93, pp. 926-932, Sep. 2015.

[43] L. Chung, J. H. J. Kim, and S. T. Yi, "Bond strength prediction for reinforced concrete members with highly corroded reinforcing bars," *Cement. Concrete. Comp.*, vol. 30, no.7, pp. 603-611, Aug. 2008.

[44] L. Jin, M. Liu, R. Zhang, and X. Du, "3D meso-scale modelling of the interface behavior between ribbed steel bar and concrete," *Eng. Fract. Mech.*, vol. 239, Nov. 2020, Art. no. 107291.

[45] A. A. Almusallam, A. S. Al-Gahtani, A. R. Aziz, and Rasheeduzzafart, "Effect of reinforcement corrosion on bond strength," *Constr. Build. Mater.*, vol. 10, no.2, pp. 123-129, Mar. 1996.